

## Novel in situ and ex situ techniques for the study of lithium/electrolyte interfaces

Guorong Zhuang<sup>a</sup>, Kuilong Wang<sup>a</sup>, Gary Chottiner<sup>a,\*</sup>, Rachael Barbour<sup>b</sup>, Yuyan Luo<sup>b</sup>, In Tae Bae<sup>b</sup>, Donald Tryk<sup>b</sup>, Daniel A. Scherson<sup>b,\*</sup>

<sup>a</sup> Department of Physics, Case Western Reserve University, Cleveland, OH 44106, USA

<sup>b</sup> Department of Chemistry, Case Western Reserve University, Cleveland, OH 44106, USA

### Abstract

Various aspects of the reactivity of lithium toward propylene carbonate (PC) and poly(ethylene oxide) (PEO) have been examined using ex situ and in situ spectroscopic techniques, respectively. Temperature programmed desorption of perdeuterated PC ( $d_6$ -PC) layers condensed at about 150 K on a clean Li film supported on an Au foil yielded a broad  $m/e$  peak, at temperatures in the range from 220 to 520 K (and thus much lower than that found for  $\text{Li}_2\text{CO}_3$ ), which was tentatively ascribed to the thermal decomposition of a lithium alkyl carbonate. A spectroelectrochemical cell/environment controlled chamber has been designed and constructed to examine Li/PEO( $\text{LiClO}_4$ ) electrolyte interfaces formed by Li electrodeposition on to a thin Au layer sputtered on the surface of a Ge internal reflection element in situ using attenuated total reflection Fourier-transform infrared (ATR/FT-IR) spectroscopy. This assembly enables variable temperature measurements to be performed under conditions of utmost cleanliness. Preliminary results have indicated that in the case of PEO/ $\text{LiClO}_4$  this ATR/FT-IR technique has sufficient sensitivity to observe changes in the composition of the surface and near surface region, including reaction products and perchlorate anions, which contribute to the transport of charge in the electrolyte phase.

*Keywords:* Lithium/electrolyte interfaces

### 1. Introduction

A better understanding of the physicochemical properties of the passive film on Li in non-aqueous media, including both liquid and Li-ion conducting solid polymer electrolytes, is expected to provide insight into the factors that control the rechargeability of secondary Li-based battery systems [1]. Efforts in this laboratory have been focused on the use of an array of complementary ex situ and in situ spectroscopies for the characterization of the chemical, electronic and vibrational properties of Li/electrolyte interfaces. The techniques employed include: ex situ Auger electron (AES), X-ray photoelectron (XPS), and Fourier-transform infrared (FT-IR) spectroscopies, and temperature programmed desorption (TPD), and in situ FT-IR. This work presents results for the application of:

(i) ex situ AES and TPD for the study of propylene carbonate (PC) condensed on ultrathin, vapor-deposited Li films supported on clean polycrystalline Au,

(Au(poly)), foils in ultrahigh vacuum (UHV) environments, and

(ii) in situ attenuated total reflection Fourier-transform infrared (ATR/FT-IR) for the characterization of electrodeposited Li films from  $\text{Li}^+$ /poly(ethylene oxide) (PEO) solid polymer electrolytes on to a thin layer of Au (about 5 nm) sputtered on the surface of a Ge internal reflection element.

### 2. Assembly and characterization of lithium/propylene carbonate passive films in ultrahigh vacuum environments

The physicochemical properties of the passive film on Li in non-aqueous electrolytes are believed to be governed largely by the nature of the products of the chemical and/or electrochemical reactions between metallic Li and the solvent, the salt anion, either as a fully solvated or ion-paired species, and impurities present in the electrolyte, such as water and other atmospheric components [2–4].

\* Corresponding authors.

One of the strategies developed in this laboratory aimed at gaining insight into the chemical composition of these passive films involves the use of surface analytical techniques for the assembly and characterization of ultraclean Li/electrolyte interfaces in UHV. This procedure involves the sequential deposition and condensation of Li and the solvent on to a host substrate to simulate conventional electrochemical interfaces comprising the same constituents. The virtues of this approach are numerous. Specifically, UHV offers conditions of utmost cleanliness for the synthesis and surface analysis of Li/solvent interfaces, making it possible to examine in detail the effects of gas-phase impurities on the reaction products. In addition, the combined use of electron-, and photon-based spectroscopic techniques, and TPD, enables various aspects of the interface to be probed in UHV with a high degree of specificity and sensitivity.

A particularly intriguing aspect of this approach is the fact that the work function–electrochemical potential correlation suggests that the potential across the Li/frozen solvent interface is closely related to that of an unpolarized Li electrode in contact with a liquid electrolyte involving the same solvent. Hence, the interfacial reactivity of the bare Li surface toward the frozen solvent (except for kinetic hindrances derived from differences in temperature) should resemble that of a Li electrode immersed in that electrolyte at open circuit, i.e., in situ conditions. It is conceivable, albeit not as yet attempted, to co-adsorb, with the solvent, electrolyte salts exhibiting reasonable vapor pressure during the assembly of these Li/non-aqueous solvent interfaces to obtain basic information regarding the reactivity of the anion toward metallic Li in the presence of the solvent. It is unlikely, however, that this procedure would render solvated ions, as in the case of solutions involving high dielectric constant solvents. This factor could be responsible for differences in the physicochemical properties of reaction layers formed in the two environments.

The first section of this work illustrates the application of this multitechnique approach to the study of the reactivity of metallic Li toward PC in UHV by condensing perdeuterated PC ( $d_6$ -PC) on to a thin layer of Li vapor deposited on the surface of a clean polycrystalline Au substrate (Au(poly)) at cryogenic temperatures.

### 3. Experimental

All measurements were conducted in two independent UHV chambers described earlier in the literature operating at pressures of about  $2 \times 10^{-10}$  torr [5,6].

#### 3.1. Lithium deposition

Lithium was evaporated from properly degassed SAES Getters sources on to an Au(poly) foil kept at

110 K, which had been cleaned by a series of  $\text{Ar}^+$  bombardment/thermal annealing cycles. The purity of the Li layer was assayed with AES and XPS during the calibration of each of the sources to identify the possible presence of carbon and oxygen impurities. Once a source was found to produce clean Li in a controlled fashion, the freshly deposited films were exposed to PC in the gas phase without prior AES characterization, a procedure that minimizes the risk of contamination with adventitious gases in the chamber [6].

Lithium coverages are given in terms of percent of AES signal (%Li), where  $\%Li = (I_{Li}/S_{Li}) / (I_{Li}/S_{Li} + I_{Au}/S_{Au})$ ,  $I_i$  is the peak-to-peak height of the AES signal, and  $S_i$  is the sensitivity factor of element  $i$ . The equivalent thickness of the Li deposits was estimated based on the homogeneous attenuation of the Au AES signal via the equation  $I = I_0 \exp(-x/\lambda)$ , where  $\lambda$  is the mean free path of AES electrons for Au, i.e., about 1 nm. The density of Li is  $0.53 \text{ g cm}^{-3}$ , which corresponds to an atomic density of  $4.57 \times 10^{22} \text{ atoms cm}^{-3}$ , i.e., a 78% Li layer has an equivalent thickness of about 1.6 nm.

#### 3.2. Propylene carbonate

Perdeuterated PC (Icon Corporation,  $\text{C}_4\text{O}_3\text{D}_6$ , mass = 108 amu), denoted as  $d_6$ -PC, was used for all TPD measurements to avoid ambiguities in the interpretation of the TPD data derived from the presence of dihydrogen in the UHV chamber (the major background gas impurity in UHV). Prior to the actual experiments,  $d_6$ -PC was purified by a series of freeze/thaw cycles to remove high vapor pressure residual gases (mostly  $\text{CO}_2$  and CO, see below) followed by pumping, while keeping the solvent at 200 K using an external alcohol/dry-ice bath.

Ultrapurified  $d_6$ -PC was admitted into the UHV chamber via a doser incorporating a capacitance manometer and a multicapillary array facing the sample. During the dosing, all filaments, including the mass spectrometer, were turned off to avoid decomposition. These effects are illustrated in Fig. 1, which compares the  $m/e = 80$  TPD spectra obtained after dosing a clean Au(poly) surface at 150 K with 0.23 L and 0.1 L  $d_6$ -PC with the mass spectrometer filament off (curve A) and on (curve B), respectively. As clearly indicated, the hot filament induces the partial fragmentation of PC yielding TPD features not found for the neat species.

The fragmentation pattern of ultraclean  $d_6$ -PC was determined from the TPD spectra of a thick layer of the material ( $\sim 10$  L to 30 L) condensed at about

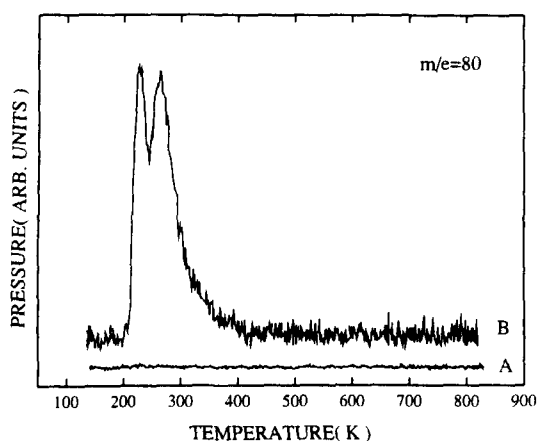


Fig. 1. TPD ( $m/e = 80$ ) spectra obtained after dosing a clean Au(poly) foil at 150 K with 0.23 L and 0.1 L  $d_6$ -PC with the mass spectrometer filament off (curve A) and on (curve B), respectively. Heating rate:  $3 \text{ K s}^{-1}$ .

160 K on a clean Au foil which had never been exposed to Li. As found in this laboratory, this temperature is high enough to prevent CO and  $\text{CO}_2$  from adsorbing on bare Au(poly). Two sets of five  $m/e$  values were traced in each of the runs until the ratios of the various fragments were stabilized. Ultrapurified gaseous  $d_6$ -PC kept in the stainless-steel doser lines for a few hours undergoes spontaneous decomposition to generate CO and  $\text{CO}_2$  as the major impurities. Over a period of a few days, ultrapurified PC left in the doser was found to decompose further, yielding, in addition to CO and  $\text{CO}_2$ , a new TPD  $m/e = 80$  peak attributed to  $\text{C}_3\text{D}_6\text{O}_2$  centered at 210 K not observed for freshly purified PC.

The cracking pattern of condensed, bulk-like, ultrapurified PC, was similar to that of ultrapurified PC introduced in the chamber directly from the doser, except that in the latter case the relative amounts of CO and  $\text{CO}_2$  (compared with other PC fragments) were found to be much larger. This effect is due to the PC-induced desorption of these gases from the walls of the chamber or reactions with stainless steel (see above). For these reasons, the doser was repeatedly flushed with PC before acquisition of a set of TPD spectra.

TPD spectra were recorded for the most prominent  $d_6$ -PC fragments identified from a survey of  $m/e$  values in the range 1–110, including  $m/e = 108, 90, 64, 44, 34$ . Also collected were spectra for  $m/e = 4$  ( $\text{D}_2$ ), and  $m/e = 32, 28, 20, 18, 42, 40$ , and 2 to identify the possible formation of carbonate and hydroxide species arising from reactions involving Li and adventitious gases in the chamber such as oxygen and water.

### 3.3. Assembly and characterization of Li/PC layers

Lithium/propylene carbonate interfaces were formed by dosing  $d_6$ -PC to the desired level immediately after deposition of the Li layer. This procedure avoids ex-

tended exposure of the highly reactive film to adventitious gases in the UHV chamber and therefore decreases the degree of contamination.

## 4. Results and discussion

Fig. 2 compares the  $m/e = 44$  TPD spectra for 4 L of  $d_6$ -PC condensed on bare Au(poly) (curve A) and Li-covered Au(poly) (curve B). As clearly shown, the presence of Li gives rise to a broad peak extending from about 220 to about 520 K and two smaller peaks centered about 750 and about 860 K. The prominent peak at about 230 K observed for the bare Au(poly) surface (see curve A) is due to the sublimation of bulk-like  $d_6$ -PC. Also barely noticeable in this curve is a small feature overlapping the tail of the large peak. Based on a more comprehensive set of  $m/e$  TPD spectra obtained in the range of small  $d_6$ -PC coverages not shown in this work, this feature has been tentatively attributed to  $d_6$ -PC adsorbed directly on the Au surface. The high temperature  $m/e = 44$  peaks 700–900 K, observed in the case of  $d_6$ -PC condensed on Li/Au(poly) can be attributed to the thermal decomposition of  $\text{Li}_2\text{CO}_3$ . Evidence in support of this view was obtained by experiments involving exposure of Li/Au(poly) to  $\text{CO}_2$ , for which the  $m/e = 44$  TPD spectra showed peaks at about the same temperature. The broad feature observed in curve B, Fig. 2, can be tentatively ascribed to the thermal decomposition of a lithium alkyl carbonate formed by the reaction of PC with Li, for which  $\text{CO}_2$  is expected to be released at a much lower temperature than the corresponding inorganic carbonate. Efforts to verify this assignment are currently underway in this laboratory by examining the  $m/e = 44$  spectra of a genuine alkyl carbonate prepared in UHV by exposing to  $\text{CO}_2$  a layer of Li alkoxide formed by the adsorption of an alcohol on to the Li surface. It must be stressed

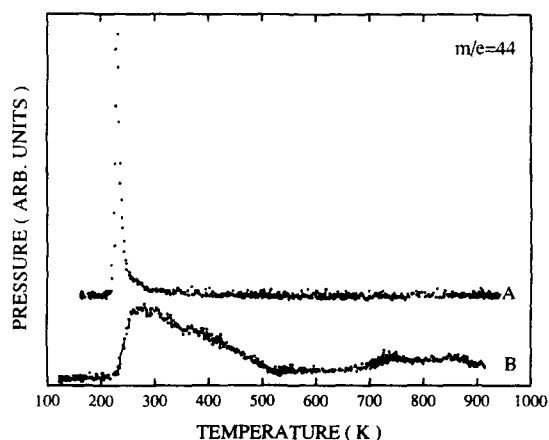


Fig. 2. TPD ( $m/e = 44$ ) spectra for 3 L and 4 L  $d_6$ -PC condensed at 120 K on nominally on bare Au(poly) (curve A) and on a 78% Li-covered Au(poly) (curve B), respectively. Heating rate:  $3 \text{ K s}^{-1}$ .

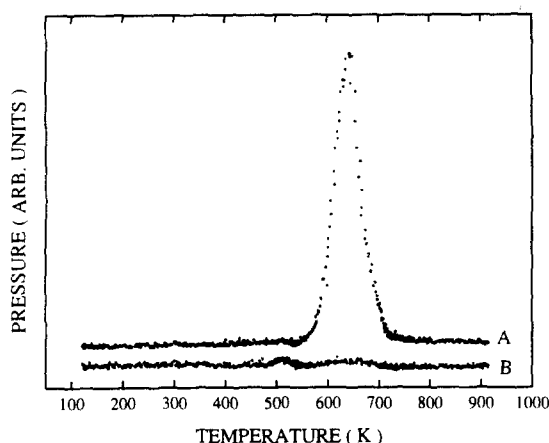


Fig. 3.  $m/e=4$  (curve A) and  $m/e=2$  (curve B) TPD spectra for 4.6 L  $d_6$ -PC condensed at about 110 K on Li-covered Au(poly). Heating rate:  $3 \text{ K s}^{-1}$ .

that the formation of alkyl carbonates in electrochemical environments has been proposed by Aurbach et al. [3] on the basis of in situ external reflection studies performed in PC electrolytes. If the suggested assignment of the broad feature in the TPD proves to be correct, a link between in situ and ex situ measurements on this type of system could be established.

The  $m/e=4$  TPD spectra displayed a desorption peak at about 650 K, which could correspond to the thermal decomposition of LiD (see curve A, Fig. 3). A similar feature was also observed in similar studies in this laboratory involving the reactivity of Li toward condensed perdeuterated THF (TDF), but was not found for PC or TDF adsorbed on polycrystalline Au or Ag never exposed to Li. It may be noted that both  $\text{H}_2$  and  $\text{D}_2$  react with Li at room temperature to form the corresponding hydride or deuteride. It seems therefore conceivable that the LiH or LiD could be formed by a reaction between  $\text{H}_2$  and  $\text{D}_2$  desorbed from the chamber walls during PC dosing. However, despite the fact that the partial pressure of  $\text{H}_2$  in the chamber is two orders of magnitude larger than that of  $\text{D}_2$ , and given that the chemical reactivity of the two species to produce the hydride (or deuteride) can be assumed to be the same, the  $m/e=2$  recorded during the same TPD run (see curve B, Fig. 3) yielded only a very small peak at about the expected decomposition temperature of the hydride. It may thus be concluded that  $\text{D}_2$  originates from PC adsorbed on Li and not from other sources. A series of peaks with other  $m/s$  values were observed in the TPD curves centred at about 650 K. On this basis, a more likely source of  $\text{D}_2$  in the TPD may be the thermally induced dehydrogenation of one (or more) adsorbed reaction products.

## 5. In situ attenuated total reflection/Fourier-transform infrared spectroscopy (ATR/FT-IR) at the metallic lithium/poly(ethylene oxide) interface

The possibility of replacing liquid electrolytes by  $\text{Li}^+$ -conducting solid polymer electrolytes is expected to simplify the design and manufacturing of Li-based batteries as well as to improve their overall rechargeability [7]. Such gains in performance are assumed to be derived from the low reactivity of certain solid polymer electrolytes, particularly PEO, toward metallic Li.

Insight into some of these issues has been gained using in situ ATR/FT-IR spectroscopy as a probe of the vibrational properties of the interface [8,9]. Crucial to the success of these experiments was the design and construction of a sandwich-type, variable-temperature spectroelectrochemical cell, which fits inside a portable, custom-made, environment-controlled chamber. This approach makes it possible to transfer the cell from the glove box to the FT-IR spectrometer, either under vacuum (0.1 mtorr) or in ultrahigh purity (UHP) argon, without exposure to the atmosphere. Ultraclean Li/PEO(LiX), (where  $\text{X} = \text{ClO}_4^-$ ,  $\text{AsF}_6^-$ ,  $\text{PF}_6^-$ ,  $\text{CF}_3\text{SO}_3^-$  or other suitable counter-ions) interfaces are produced in situ by electrodepositing Li from the PEO(LiX) electrolyte on to a thin Au electrode sputtered on the surface of a Ge internal reflection element under highly uniform current distribution conditions. The spectral features associated with the reaction products of Li and PEO, including possible contaminants, such as water, dioxygen and carbon dioxide, can be observed by comparing the ATR/FT-IR spectra obtained prior to Li deposition with that recorded after electrodeposition and stripping of metallic Li. This spectroelectrochemical cell/environment-controlled chamber assembly can be employed in studies involving a variety of solid polymer electrolytes including proton-conducting materials, such as Nafion, under a controlled atmosphere, and over a wide range of temperatures.

This section will provide a detailed description of the spectroelectrochemical cell/environment-controlled chamber and present some preliminary in situ ATR/FT-IR results obtained for the Li/(PEO/LiClO<sub>4</sub>) system at 55 °C, as a function of the applied potential.

### 5.1. Description of the spectroelectrochemical cell and environment-controlled chamber for in situ ATR/FT-IR studies of Li/PEO(LiClO<sub>4</sub>) interfaces

The variable-temperature spectroelectrochemical cell assembly consists of a series of flat components placed adjacent to each other to form a sandwich-type arrangement within a U-shaped brass block (see Fig. 4). These include in sequence: a Cu-supporting plate; a Ge prism internal reflection element (IRE; 50 mm × 20

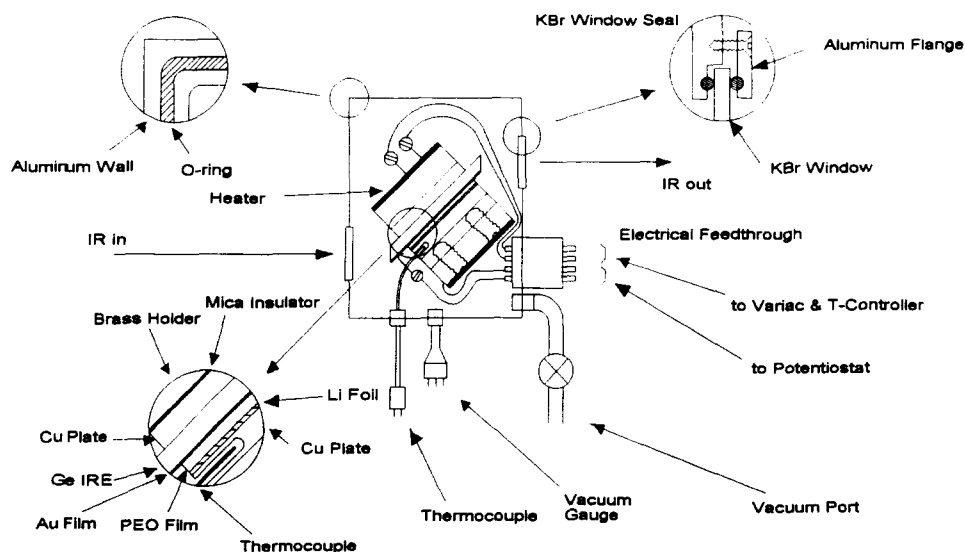


Fig. 4. Schematic diagram of the spectroelectrochemical cell/environment-controlled chamber for studies of Li-solid polymer electrolyte interfaces. IRE = internal reflection element.

mm,  $45^\circ$ ) covered with a layer of Au (about 5 nm thickness), which is used as the semitransparent working electrode, sputtered on the face of the internal reflection element exposed to the PEO electrolyte (a thicker (100 nm) Au layer in the form of a U (not shown in this Figure) was sputtered around the perimeter of the same face to increase the conductivity between the working electrode and the current collector); the PEO film (60  $\mu\text{m}$ ), which covers the width of the internal reflection element; a Li ribbon counter-reference electrode, (Li[C/R]); a second Cu-supporting plate, which serves as the current collector for the Li[C/R]. A layer of Ni was sputtered on to this plate to prevent possible alloy formation between Cu and Li. Unlike the design described in a previous paper [9], the present cell arrangement cell does not require the use of a spacer.

The working electrode (active area: about  $6\text{ cm}^2$ ) is electrically isolated from the brass block by means of a thin piece of mica. A hole (1.8 mm diameter) was drilled in one side of the Cu plate adjacent to the Li ribbon to house a K-type thermocouple junction used to monitor the temperature of the cell.

The cell assembly is placed into a U-shaped brass block holder, and is fixed in position by means of two bolts. The entire unit is then inserted via two pins into a Kel-F piece (not shown in this Figure) attached to the bottom of the environment-controlled aluminum chamber, which provides both thermal and electrical isolation.

A Cu–Be–Au spring wire is used to make contact with the Au–Ge working electrode. The electrical connection to the Li[C/R] electrode is made via the brass block with an Au spring-loaded contact inserted into the Kel-F piece (see Fig. 4).

Once all the connections are made, a U-shaped heating unit (not shown in the Figure) consisting of a Kapton encapsulated resistive element (Omega, 200 W, 115 V a.c.) adhered to a thermal insulator (Carborundum) placed in an aluminum housing is slipped over the whole cell assembly. The temperature is controlled by a West 800 temperature controller.

The environment-controlled chamber (see Fig. 4) is a rectangular box, which can be isolated from the atmosphere by means of an O-ring compressed lid, and contains a series of orifices used to house two O-ring-sealed KBr windows (1 in. diameter, 5 mm thick, International Crystal), electrical feedthroughs (MCD) for the heater, the electrochemical cell and the thermocouple, a vacuum port and a thermocouple vacuum gauge.

The complete cell/environment-controlled chamber unit is fully assembled in the dry box (Vacuum Atmospheres) under UHP argon atmosphere and then transferred to the spectrometer. A piece of freshly cut metallic Li is often placed inside the environment-controlled chamber to remove gas-phase contaminants due to possible small leaks.

## 5.2. Purification of poly(ethylene oxide)

Poly(ethylene oxide) (Aldrich, mol. wt. = 600 000) was purified by dialysis to remove Ca (about 0.003%) derived from traces of the polymerization initiator (calcium amide) and other impurities. The cellulose dialysis bags (Sigma, Chem. Co.), were cleaned by first rinsing with distilled water followed by boiling in a one to one ethanol/water mixture for 1 h and finally rinsing again with distilled water. The PEO was placed in the bags and dialyzed in water for 48 h, changing the solvent

every 2–3 h the first day, and every 4–5 h the second day. After this procedure was completed the PEO/water solution was evaporated to dryness in a Rotavap.

Poly(ethylene oxide) film electrolytes were prepared with ultrapurified PEO/LiClO<sub>4</sub> solutions as described elsewhere [9], except that the films were dried in a vacuum desiccator equipped with heating capabilities installed inside the glove box using a calibrated Variac and a thermocouple to set the appropriate temperature. In this fashion, the PEO films are never exposed to the ambient atmosphere.

### 5.3. Infrared spectroelectrochemistry

The ATR/FT-IR spectra were acquired with a resolution of 4 cm<sup>-1</sup> (i.e., one point every 2 cm<sup>-1</sup>) in an IBM IR-98 instrument equipped with an MCT detector. All spectra presented in this work represent the average of the co-addition of 200 interferometric scans recorded while scanning the potential at 1 mV s<sup>-1</sup>, normalized by the (average) spectrum recorded at a fixed potential of 1.8 V prior to the initiation of the scan.

Spectroelectrochemical measurements were performed with PEO/LiClO<sub>4</sub> films with a concentration of Li salt equivalent to one Li<sup>+</sup> per 36 (–CH<sub>2</sub>–CH<sub>2</sub>O–) units at a constant temperature of 55 °C. During the spectral collection, the environment-controlled chamber was evacuated to about 10<sup>-2</sup> torr and the sample compartment of the IBM-98 was purged continuously with N<sub>2</sub> (Gas Techniques). Cyclic voltammetry were obtained with a PAR Model 173 potentiostat a PAR Model 175 programmer and a custom-made data acquisition system.

## 6. Results and discussion

A typical cyclic voltammogram of the Au/Ge electrode in PEO/LiClO<sub>4</sub>, recorded at 55 °C in the spectroelectrochemical cell is shown in Fig. 5 (other conditions are specified in the Figure caption). This curve is very similar to those obtained using a thick layer of Au (200–500 nm) sputtered on glass as the working electrode under otherwise identical experimental conditions. The prominent peaks observed in the scan in the negative and positive directions correspond to the deposition and stripping of metallic Li, respectively. The fact that the charge associated with the deposition is larger (405 mC) than that obtained upon stripping (375 mC) may be ascribed to a chemical reaction that consumes irreversibly a fraction of the freshly deposited metallic Li. As may be inferred from the results shown in this Figure, the reference potential is shifted in the negative direction about 0.2 V with respect to a reversible Li/Li<sup>+</sup> electrode in the same PEO electrolyte. This phenomenon is most probably due to polarization effects

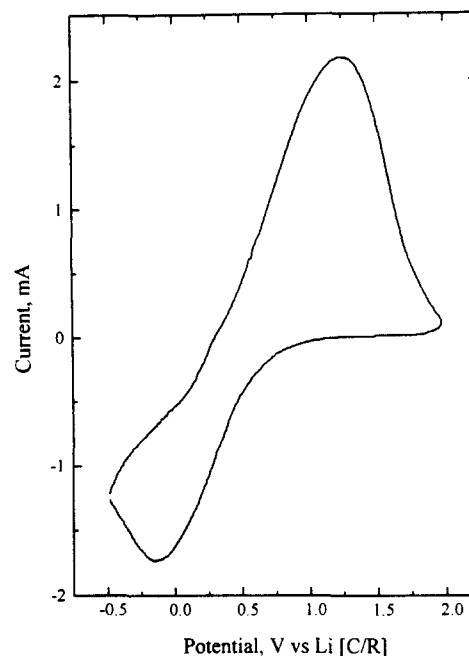


Fig. 5. Cyclic voltammogram of a thin Au layer (5 nm) sputtered on the surface of a Ge internal reflection element in PEO/LiClO<sub>4</sub>, 1 Li<sup>+</sup>/36 (–CH<sub>2</sub>–CH<sub>2</sub>O–) electrolyte obtained in the spectroelectrochemical cell at 55 °C after the electrode had been cycled three times between the specified limits. Electrode area: about 6 cm<sup>2</sup>; scan rate: 5 mV s<sup>-1</sup>.

associated with the Li[C/R]. Evidence in support of this view was obtained from experiments involving a three-electrode thin layer cell, for which the overall voltammetric features were virtually the same as those shown in Fig. 5.

Since the main emphasis of this work is focused on modifications in the vibrational properties of the interface induced by the contact of ultraclean Li with the PEO electrolyte, this potential shift is not expected to introduce major complications in the analysis of the data.

Fig. 6 shows a series of potential difference ATR/FT-IR spectra obtained from the Au/Ge electrode in PEO/LiClO<sub>4</sub> in the spectroelectrochemical cell at 55 °C during the first voltammetric cycle at 1 mV s<sup>-1</sup> (see Fig. 7). As noted earlier, the spectra recorded at 1.8 V before initiation of the (first) scan was used as a reference. The values specified in each curve represent the average (scanned) potential over which the spectra were collected. These spectra display a number of both negative-, and positive-pointing peaks, particularly in the region between 780 and 1800 cm<sup>-1</sup>, as seen in the expanded scale in Fig. 8. Close inspection of these spectral data and the cyclic voltammogram in Fig. 7 reveals a direct correlation between the flow of charge through the electrode and the magnitude of the peaks in the potential region between 1.68 and 0.57 V. Most of the bands below 800 cm<sup>-1</sup> are due to Ge and will not be discussed further here.

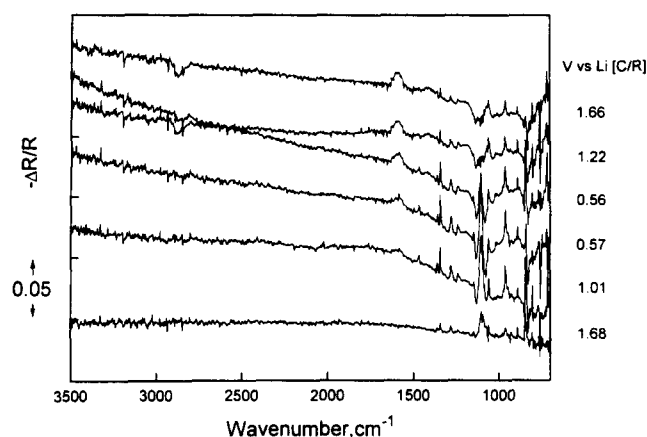


Fig. 6. Series of potential difference ATR/FT-IR spectra obtained for the Au/Ge electrode in PEO/LiClO<sub>4</sub> in the spectroelectrochemical cell at 55 °C during the first voltammetric cycle at 1 mV s<sup>-1</sup> shown in Fig. 7 using as a reference the spectra recorded at 1.8 V vs. Li[C/R], prior to the initiation of the scan.

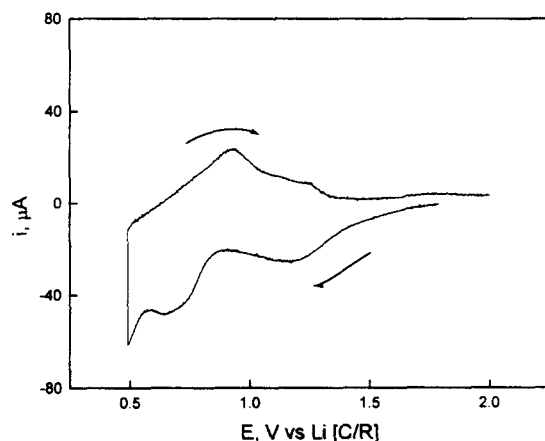


Fig. 7. First cyclic voltammogram of a Au/Ge electrode in PEO/LiClO<sub>4</sub> obtained in the spectroelectrochemical cell at 55 °C. Electrode area: 5 cm<sup>2</sup>; scan rate: 1 mV s<sup>-1</sup>.

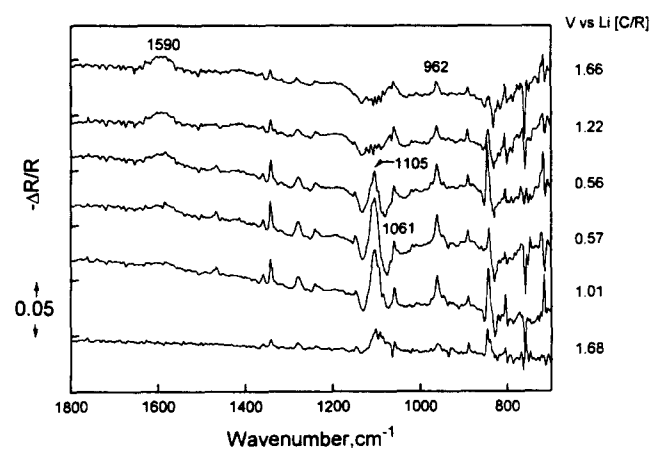


Fig. 8. Expanded view of the potential difference spectra in Fig. 6 in the region 700–1800 cm<sup>-1</sup>.

### 6.1. Spectral assignment

With the exception of the peak centered at about 1590 cm<sup>-1</sup> all positive-pointing features are characteristic of PEO, as evidenced by a comparison of these spectra with that of a PEO electrolyte film of the same composition obtained with the Ge internal reflection element prism at two different temperatures (see Fig. 9). The fact that these peaks are positive-pointing implies an increase in the amount of PEO probed by the beam as the potential is scanned in the negative direction. This effect is most likely due to an increase in the effective density of pure PEO induced by the temporal loss of LiClO<sub>4</sub> from the immediate vicinity of the working electrode [10]. Such a process is brought about by the underpotential deposition of Li<sup>+</sup> on to the Au electrode, which is accompanied by the migration of ClO<sub>4</sub><sup>-</sup> into the bulk electrolyte to preserve electroneutrality. Two additional observations lend support to this explanation. First, the intensity of the bands in question decrease as the underpotential deposited layer is stripped from the surface during the scan in the positive direction, and second, the bipolar character of the band at about 1107 cm<sup>-1</sup> is consistent with the superposition of a positive-pointing band, due to PEO, and a negative-pointing band ascribed to (electrolyte phase) perchlorate ion.

Particularly interesting is the positive-pointing feature centered at 1590 cm<sup>-1</sup>, which is generated irreversibly during the scan in the negative direction. Whether this yet be assigned feature is associated with a reaction between metallic Li and PEO or an impurity present in the PEO film has not as yet been resolved.

Although this and various other aspects of the in situ spectroelectrochemical data obtained in this study still remain to be elucidated, the results so far obtained clearly illustrate the extraordinary degree of sensitivity

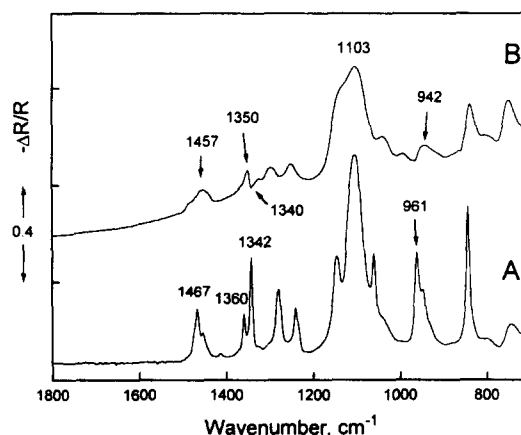


Fig. 9. ATR/FT-IR spectra of a film of PEO prepared under identical conditions as the PEO/LiClO<sub>4</sub> electrolyte used in the spectroelectrochemical experiments using a Ge internal reflection element at two different temperatures, i.e., 23 and 67 °C.

and versatility of this methodology for the study not only of Li/PEO but a more general class of electrode solid polymer electrolyte interfaces. On this basis, a systematic application of in situ ATR/FT-IR techniques, now in progress in this laboratory, will contribute to a better understanding of the chemistry and electrochemistry of Li in Li<sup>+</sup>-conducting solid polymer electrolytes.

## 7. Conclusions

The combined use of a carefully selected array of in situ and ex situ techniques, as illustrated by the studies presented in this paper, is expected to help elucidate important physicochemical aspects of the passive film on Li and thereby provide rational guidelines for the development of new electrolytes for Li-based battery systems.

## Acknowledgements

This work was supported by the Department of Energy, Basic Energy Sciences and by the Lawrence

Berkeley Laboratory through a subcontract from the Department of Energy.

## References

- [1] J.P. Gabano (ed.), *Lithium Batteries*, Academic Press, New York, 1983; H.V. Venkatesetty (ed.), *Lithium Battery Technology*, Wiley, New York, 1984.
- [2] J. Peled, *J. Electrochem. Soc.*, 134 (1987) 273.
- [3] D. Aurbach, M.L. Daroux, P.W. Faguy and E. Yeager, *J. Electrochem. Soc.*, 7 (1987) 1611.
- [4] D. Aurbach, Y. Gofer, M. Ben-Zion and P. Aped, *J. Electroanal. Chem.*, 339 (1992) 451.
- [5] P. Herrera-Fierro, K. Wang, F.T. Wagner, T.E. Moylan, G.S. Chottiner and D.A. Scherson, *J. Phys. Chem.*, 96 (1992) 3788.
- [6] K. Wang, G.S. Chottiner and D. Scherson, *J. Phys. Chem.*, 97 (1993) 11075, and refs. therein.
- [7] J.R. McCallum and C.H. Vincent (eds.), in *Polymer Electrolyte Reviews*, Elsevier Applied Science, Barking, UK, 1987.
- [8] B.W. Johnson and K. Doblhofer, *Electrochim. Acta*, 38 (1993) 695.
- [9] T. Ichino, B.D. Cahan and D.A. Scherson, *J. Electrochem. Soc.*, 138 (1991) L59.
- [10] I.T. Bae, X. Xing, E.B. Yeager and D.A. Scherson, *Anal. Chem.*, 61 (1989) 1169.